Journal of Sound and Vibration (2000) **231**(5), 1383–1395
doi:10.1006/jsvi.1999.2471, available online at http://www.idealibrary.com on IDEAL®

VIBRATION ANALYSIS OF WIRE AND FREQUENCY RESPONSE IN THE MODERN WIRESAW MANUFACTURING PROCESS

SONGBIN WEI AND IMIN KAO

Department of Mechanical Engineering, State University of New York at Stony Brook, Stony Brook, NY 11794-2300, *U.S.A.*

(*Received* 11 *September* 1998, *and in final form* 24 *May* 1999)

1. INTRODUCTION

Wiresaw manufacturing is an emerging technology for wafer production in semiconductor and photovoltaic industries because of its ability to cut large ingot into thick or very thin wafers with small kerf loss and high yield [1–3]. The wiresaw employs a steel wire with abrasive slurry to cut through silicon ingot [2]. Since a high-speed wire with abrasive slurry is employed in the wiresaw manufacturing process, understanding the vibration behavior of the system is very pivotal in the prediction of dynamic behaviors and kerf loss* of the cutting process.

The vibration analysis of a moving wire has been studied by many researchers. An extensive review can be found in reference [4]. The vibration of wire is modelled as the transverse vibration of an axially moving string under tension. Modal analysis was presented [5, 6] to find the eigenfunctions and natural modes. Recent research has been extended to vibration of axially accelerating string [7], damped string vibration system [8], and the active vibration control [9]. The applications of research can be found in diverse mechanical systems such as high-speed magnetic and paper tapes, high speed fiber winding, thread lines, band saws, pipes that contain flowing fluid and power transmission chains and belts.

The wire employed in wiresaw, however, is characterized by its low mass density (very thin wire, typically 175 μm in diameter, with low mass per unit length) and high tension. These two important features result in very high critical speed for stability, making the system stable. The excitations to the wire are provided through the contact of abrasives via the "rolling-indenting" process [3]. Therefore, our research interests for wiresaw vibration are primarily focused on the amplitude of the vibration subject to different operating parameters such as tension and speed of the wire. Frequency response is used to examine the amplitude of vibration under a spectrum of excitation frequencies.

*Kerf loss refers to the materials removed during the slicing process to make wafers from ingot. A cost-effective process requires minimal kerf loss.

0022-460X/00/151383 + 13 $35.00/0 © 2000 Academic Press

In this paper, a new study and application of wire vibration in the wiresaw manufacturing process with abrasive slurry in free abrasive machining (FAM) is presented. First, we employ the equation of motion for the wire under the boundary conditions due to the constraints of the wiresaw manufacturing process. Secondly, we reviewed the modal analysis with closed-form solution. The responses of harmonic excitations, applied by both single and multiple particles, are presented. Numerical results using the Galerkin's method are compared with those of the closed-form solutions. Frequency response with different wire translating velocities and tensions are investigated. The results show that the frequency responses are almost identical for speeds between 0 and 25 m/s under a typical wire tension of 20 N. However, the variations in tension have a very pronounced effect on the frequency response. These results suggest important strategies in the design of wiresaw. Since the damping effect of slurry also plays a role in the vibration behavior, we also study the amplitudes of vibration with respect to different damping factors due to the abrasive slurry.

2. MODELLING OF WIRESAW VIBRATION AND RESPONSE

In the wiresaw manufacturing process, the wire moves at high speed (5–15 m/s) with respect to the specimen (e.g., silicon ingot). The abrasives in the slurry are caught between the wire and ingot at the contact surface. The normal load along the Y direction due to the bow of wire and the hydrodynamic pressure of slurry [14] carries the abrasive particles and causes them to roll on the surface and at the same time to be constrained to indent the surface — the so-called "rolling indenting" process [1–3]. The excitation of vibration is a result of reaction forces applied by the individual abrasive particle on the wire through the rolling-indenting process.

In the following sections, the modelling of wire vibration employed in wiresaw manufacturing process is summarized with formulation and modal analysis. Responses from closed form and numerical results are presented. Frequency response of multiple excitations is also presented with implications to the design of wiresaw.

2.1. MODELLING OF WIRE VIBRATION IN WIRESAW MANUFACTURING PROCESS

The schematic of a moving wire in FAM process of modern wiresaw is shown in Figure 1. The compliant wire transports between two rotating capstans (*or wire guides*) separated by a distance L. The equation of motion can be derived using the Newtonian mechanics [10] or Hamilton's principle [11] as follows:

$$\rho(U_{TT} + 2VU_{XT} + V^2U_{XX}) - PU_{XX} = F \tag{1}$$

with boundary conditions

$$U(0, T) = 0 \quad \text{and} \quad U(L, T) = 0, \tag{2}$$

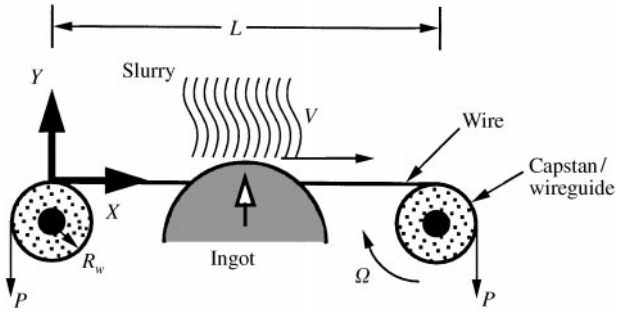

Figure 1. Schematic showing the wire and process parameters of a typical wiresaw with rotating wire guides.

where U is the transverse displacement of the wire in the Y direction, V is translating speed of the wire, P is the tension of the wire, F is the external excitation force applied on the wire per unit length, and ρ is the mass of wire per unit length.

With the introduction of dimensionless parameters $x = X/L$, $u = U/L$, $t = T\sqrt{P/(\rho L^2)}$, $f = FL/P$, $v = V\sqrt{\rho/P}$, equation (1) becomes

$$u_{tt} - 2vu_{xt} - (1 - v^2)u_{xx} = f. \tag{3}$$

2.2. MODAL ANALYSIS

Wickert and Mote [5, 6] applied the modal analysis method for discrete gyroscopic system [12, 13] to the axially moving string system and obtained a general closed-form solution for arbitrary excitations and initial conditions. The general closed-form solution is expressed in the form of an infinite series of the normal modes multiplied by time-dependent generalized co-ordinates, that is

$$\mathbf{w} = \sum_{n = \pm 1, \pm 2, \ldots} \xi_n(t)\mathbf{\Phi_n}(\mathbf{x}), \tag{4}$$

$$\mathbf{\Phi_n}(\mathbf{x}) = \begin{bmatrix} \mathrm{i}\sqrt{1 - v^2} \\ 1 \\ \hline n\pi\sqrt{1 - v^2} \end{bmatrix} \sin(n\pi x)\exp(\mathrm{i}n\pi v x), \tag{5}$$

where $\mathbf{w} = [\mathbf{u_t}\ \mathbf{u}]^{\mathrm{T}}$, $i = \sqrt{-1}$, $\xi_n(t)$ are complex generalized co-ordinates, and $\mathbf{\Phi_n}(\mathbf{x})$ are complex eigenfunctions subject to the boundary conditions in equation (2).

2.3. RESPONSE UNDER EXCITATION OF SINGLE PARTICLE

Assume the excitation is harmonic and only one particle is in contact with the wire. The dimensionless pointwise harmonic excitation can be expressed as

$$f(x, t) = f_0\delta(x - x_0)\sin(\omega t), \tag{6}$$

where f_0 is the amplitude of excitation, x_0 is the location of excitation with frequency of ω, and δ is the Dirac delta function.

2.3.1. *Closed-form solution for pointwise harmonic excitation*

Using the method in section 2.2, the steady state response for this excitation can be obtained as

$$u = f_0 \sum_{n=1}^{\infty} \frac{1}{n\pi} \frac{1}{\omega_n^2 - \omega^2} \sin(n\pi x_0) \sin(n\pi x)[(\omega_n + \omega) \sin(\omega t + n\pi v(x - x_0)) + (\omega_n - \omega) \sin(\omega t - n\pi v(x - x_0)) - 2\omega \sin(\omega_n t + n\pi v(x - x_0))], \tag{7}$$

where $\omega_n = n\pi(1 - v^2)$ with $n = 1, 2, 3, \ldots$ are the dimensionless natural frequencies of the wire.

The corresponding actual natural frequencies are

$$\Omega_n = \omega_n \sqrt{\frac{P}{\rho L^2}} = \frac{n\pi(P - \rho V^2)}{L\sqrt{\rho P}}. \tag{8}$$

The natural frequency Ω_n in equation (8) will reduce to the usual form of the natural frequencies of a stationary string when the speed of the wire, V, is zero.

From equation (8), it is obvious that the natural frequency will vanish when $V = \sqrt{P/\rho}$ which is defined as the critical speed. When the speed of the wire is near this speed, the wire will experience divergence instability. For the industrial wiresaw, the mass density ρ is very small while tension P is high (around 20–30 N) which results in a very high critical speed (typically over 300 m/s). The wiresaw operating speed is normally less than 20 m/s, hence the divergence instability is generally not a concern.

The response to the single-particle excitation is plotted with the three-dimensional figure, as shown in Figure 2(a), obtained from equation (7). The 3-D graph shown in Figure 2(a) is plotted with the following system parameters: $V = 10$ m/s, $\rho = 0{\cdot}1876$ g/m, $P = 20$ N, $L = 0{\cdot}3$ m, $x_0 = 0{\cdot}15$ m, $\omega = 0{\cdot}2\,\omega_1$ and $n = 100$. The fundamental dimensional frequency Ω_1 is 3416 rad/s.

The vibration is plotted across the span of the wire ($0 \leqslant x \leqslant 300$ mm) as a function of time. In Figure 2(a), the vibration pattern contains twin peaks. This is due to the fact that the response contains two main frequencies components — one is the excitation frequency and the other is the fundamental frequency of the wire. The two frequencies superpose on each other to render such typical response. Note that if the two frequencies become close to each other, the aliasing effect will appear.

2.3.2. *Numerical method*

Equation (3) is a partial differential equation and can be discretized using the Galerkin's method. Usually, the eigenfunctions of the system are chosen as the trial functions to minimize the error. For the axially moving string system, the eigenfunctions consist of two components: the real and imaginary parts, i.e., $\sin n\pi x \cos n\pi v x$ and $\sin n\pi x \sin n\pi v x$. In wiresaw manufacturing system, however, the non-dimensionized speed v is relatively small (e.g., $v = 0{\cdot}0306$) and can be

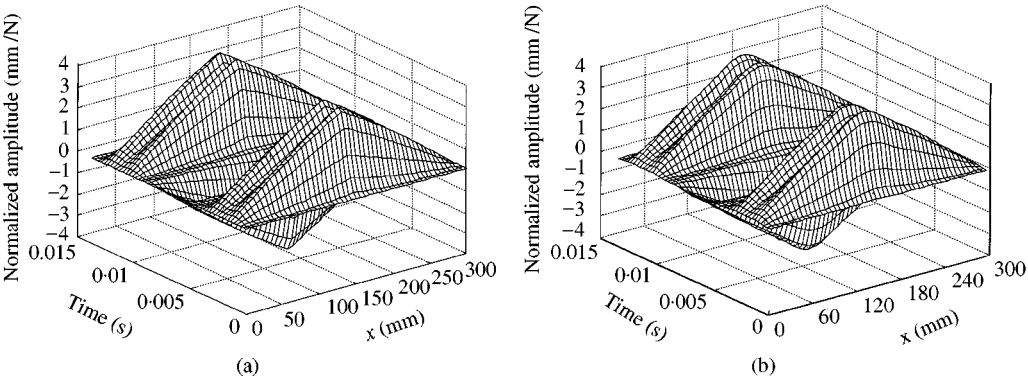

Figure 2. (a) Three-dimensional plot of the vibration analysis under a harmonic excitation of $\omega = 0{\cdot}2\omega_1$ at $x_0 = 150$ mm with normalized vibration amplitude for closed-form solution, and (b) numerical solution with Galerkin's method.

neglected. Hence, both $\cos n\pi vx$ and $\sin n\pi vx$ can be approximated as 1 and 0, respectively, at significant modes (small n). Therefore, the imaginary component can be dropped without causing much error. The resulting simplified functions, $\sin n\pi x$, happen to be the eigenfunctions of the stationary string. In the following equation, the eigenfunction of stationary string is used to form the trial function

$$u(x, t) = \sum_{j=1}^{n} q_j(t) \sin(j\pi x). \tag{9}$$

Applying the Galerkin's method, equation (3) can be discretized into simultaneous ordinary differential equations

$$\mathbf{M}\ddot{q} + \mathbf{C}\dot{q} + \mathbf{K}q = \mathbf{Q}. \tag{10}$$

The components of the matrix **M**, **C**, **K**, and the column vector **Q** are

$$m_{ij} = \begin{cases} \frac{1}{2} & \text{if } i = j, \\ 0 & \text{if } i \neq j, \end{cases}$$

$$c_{ij} = \begin{cases} 0 & \text{if } i + j = 2n, \\ \left(\dfrac{4ij}{i^2 - j^2}\right) v & \text{if } i + j = 2n + 1, \end{cases}$$

$$k_{ij} = \begin{cases} \dfrac{j^2\pi^2}{2}(1 - v^2) & \text{if } i = j, \\ 0 & \text{if } i \neq j, \end{cases}$$

$$q_i = \int_0^1 f \sin(\mathrm{i}\pi x)\, \mathrm{d}x,$$

where $i, j = 1, 2, \ldots, n$. It is obvious that **M** is a real-symmetric positive-definite mass matrix, **C** is a real-skew symmetric gyroscopic matrix, and **K** is a

real-symmetric matrix. The stiffness matrix **K** is positive definite as long as the speed of the wire is smaller than the critical speed, $V_{cr} = \sqrt{P/\rho}$. It should be noted that when $v = 0$, the matrix **C** will vanish resulting in a simplified symmetric eigenvalue system, which shows that the axially moving string system is essentially a gyroscopic system while the stationary string is not.

The solution of equation (10) can be found (for example, in reference [15]). Using the same process parameters in section 2.3.1, we set the matrix order to 10, i.e., $n = 10$. The resulting 3-D plot is shown in Figure 2(b) which is nearly identical to the results of the closed-form solution in Figure 2(a). The difference is due to (1) the use of eigenfunctions of stationary string instead of the axially moving string, (2) the numerical errors due to the finite matrix order at $n = 10$.

2.4. RESPONSE UNDER EXCITATIONS OF MULTIPLE PARTICLES

Based on the analysis of single particle excitation, we extend the vibration analysis to more realistic multiple contacts and calculate the response of such distributed excitations. We assume that the excitations are distributed over the span of the contact between the wire and the specimen, that is,

$$\sum_{j=1}^{m} f_j = \sum_{j=1}^{m} f(x_j, t) = \sum_{j=1}^{m} f_{0j}\delta(x - x_j)\sin(\omega_{f_j} t), \tag{11}$$

where m is the number of excitations each at location x_j, and f_{0j} and ω_{f_j} are the amplitude and frequency of the jth excitation respectively.

2.4.1. *Closed-form solution for multiple excitations*

The system described in equation (3) is linear if the system parameters, such as the translating speed, the mass density and tension, are constants. Therefore, the response to the excitations with multiple particles is the superposition of the response of each single particle. That is, the response can be written as

$$u = \sum_{j=1}^{m} f_{0j} \sum_{n=1}^{\infty} \frac{1}{n\pi} \frac{1}{\omega_n^2 - \omega_{f_j}^2} \sin(n\pi x_j)\sin(n\pi x)[(\omega_n + \omega_{f_j})\sin(\omega_{f_j} t + n\pi v(x - x_j)) + (\omega_n - \omega_{f_j})\sin(\omega_{f_j} t - n\pi v(x - x_j)) - 2\omega_{f_j}\sin(\omega_n t + n\pi v(x - x_j))]. \tag{12}$$

Figure 3(a) is the three-dimensional plot of the response under multiple-particle harmonic excitations with the system parameters as those in Figure 2, while a total of 100 uniformly distributed excitations are applied from $x_0 = 50$ to 250 mm.

While 100 excitations are used to plot the response in Figure 3(a), we are interested in knowing if the maximum normalized amplitude will vary under different number of excitations. Figure 3(b) presents the simulation results of the maximum normalized amplitude ranging from 1 to 200 excitations. The figure shows an immediate and appreciable drop-off in the amplitude when the number of excitations is increased. As the number keeps increasing, the amplitude approaches a constant asymptotically. From Figure 3(b), we observe that the maximum normalized amplitude does not change significantly when the number of excitation

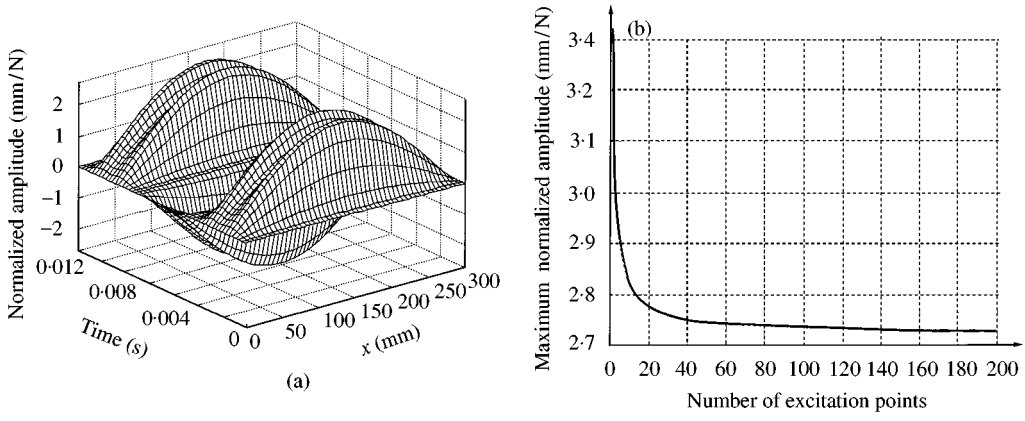

Figure 3. (a: *left*) Three-dimensional plot of the vibration analsis under multiple-particle harmonic excitations of $\omega_f = 1024$ rad/s. A total of 100 excitations distributed between $x_0 = 50$–250 mm are applied. (b: *right*) Maximum normalized amplitude versus number of excitation points. The amplitude asymptotically approaches a constant.

points exceeds 50. Therefore, a simulation of 100 excitations in Figure 3(a) is sufficient to capture the general response of a distributed vibration system of multiple excitations.

2.4.2. *Numerical solution for multiple excitations*

For multiple excitations, we can extend the numerical method in section 2.3.2. In this case, the excitation is the superposition of excitation at each point,

$$q_i = \sum_{j=1}^{m} \int_0^1 f_j \sin(i\pi x)\, dx, \tag{13}$$

where f_j is the same as that defined in equation (11). The matrix **M**, **C**, and **K** do not change since they are independent of the excitation. The results are similar to those of the closed-form solution shown in Figure 3(a).

2.5. FREQUENCY RESPONSE OF MULTIPLE EXCITATIONS

Frequency response is important in the analysis of vibration and control in practical cutting process of wiresaw. In the analysis of frequency response, the maximum normalized amplitude of vibration is obtained for a range of excitation frequencies. It is important to study the frequency response as a function of operating parameters such as the speed and tension of the wire. In this section, we present the results of frequency response of vibration with respect to wire speed and tension. The results have important implications to the design and operation of wiresaw.

Equation (12) is used for the study of the frequency response of vibration. The excitation frequency is normalized with respect to the fundamental frequency ω_1 of the wire. Without loss of generality, as we discussed in section 2.4.1, we assume

a total of 100 excitations uniformly distributed between $x_0 = 50$ and 250 mm along the wire span with the same amplitude and frequency, ω ($\omega_{f_j} = \omega$ for $j = 1 \cdots m$). The amplitude of vibration is normalized with respect to the amplitude of excitation force.

First, we assume the tension P to be a constant at 20 N. Figure 4(a) shows the frequency response obtained from equation (12), where the maximum normalized amplitude is plotted against the normalized excitation frequencies, ω/ω_1, with respect to the translating speed of wire. The plot exhibits a discontinuity when $\omega/\omega_1 = 1$, at which point the amplitude becomes infinite. Form Figure 4(a), we conclude that the maximum normalized amplitude is practically the same when the speed of wire is below 25 m/s. This is due to the small value of mass density ρ and high tension P which makes the dimensionless speed trivial when V is smaller than 25 m/s. For industrial wiresaw, the speed of a wire is normally below 15 m/s; hence, the variation in speed is not major contributing factor for vibration.

Next, we fix the wire speed at 10 m/s and vary the tension of the wire, P, from 5 to 35 N in order to explore the frequency response with respect to tension. Again, we apply equation (12) with the results plotted in Figure 4(b). The results show that the maximum normalized vibration amplitude is very sensitive to the variations of the tension. When the tension is below 10 N, the vibration amplitude is very high. The higher the tension the smaller the amplitude. The figure also shows a non-linear effect of wire tensions in the frequency response. As the tension becomes higher, further increase in tension does not result in large reduction in amplitude. Therefore, it is not advantageous to increase the tension of wire indefinitely. Besides, the maximum tension of the wire is subject to the yield strength of the material.

The results of analysis in frequency response, as shown in Figure 4(a) and (b), suggest that a more effective way to reduce vibration and kerf loss of the wiresaw

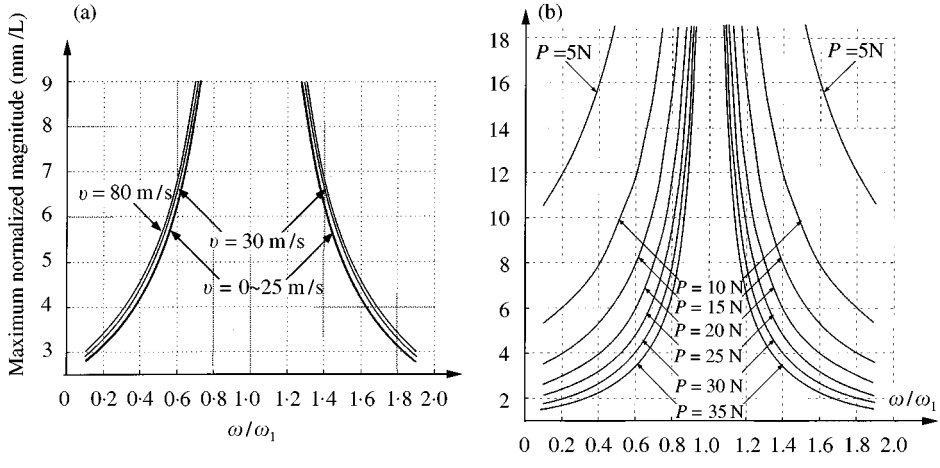

Figure 4. (a) Magnitude of the frequency response with respect to various translating speeds of wire. The speed of the wire varies from 0 to 80 m/s under a tension of 20 N (b) Magnitude of the frequency response with tension as a parameter. The tension of the wire varies from 5 N to 35 N at a wire speed of 10 m/s.

slicing process is to increase the tension of the wire, instead of the speed of the wire. Recently, the tension employed in industrial wiresaws has been increased from 15 to 30 N, resulting in considerable improvement of cutting efficiency and quality, as predicted by the results of the frequency response.

3. VIBRATION WITH DAMPING

During the wiresaw free abrasive machining (FAM) process, the high-speed wire is moving through abrasive slurry between wafer slices (refer to Figure 1). The slurry will have viscous damping effect on the wire. We assume that the damping force is linear and is proportional to the speed of the wire. Therefore, the viscous damping force can be written as

$$F_\eta(X, T) = -\eta_d(VU_X + U_T), \tag{14}$$

where η_d is generally a linear homogeneous differential operator but in this case it is assumed to be a constant for analysis, and $(VU_X + U_T)$ is the transverse velocity of the point on the wire located at X. Thus, the equation of motion becomes

$$\rho(U_{TT} + 2VU_{XT} + V^2U_{XX}) - PU_{XX} = F + F_\eta, \tag{15}$$

where F is an external distributed force excluding the damping forces.

Equation (15) can also be normalized with dimensionless parameters introduced in section 2.1, with an additional dimensionless damping factor, $\eta = \eta_d L/\sqrt{P\rho}$. Similarly, we can derive the non-dimensionalized equation of motion,

$$u_{tt} + 2vu_{xt} - (1 - v^2)u_{xx} + \eta v u_x + \eta u_t = f. \tag{16}$$

In general, closed-form solution for such damped system cannot be found [15]. Therefore, we apply numerical method to discretize the continuous equation into discrete simultaneous ordinary differential equations. When damping is included, the mass matrix **M** remains unchanged while the matrices **C** and **K** becomes

$$c_{ij} = \begin{cases} \frac{1}{2}\eta & \text{if } i = j, \\ 0 & \text{if } i \neq j \text{ and } i + j = 2n, \\ \left(\dfrac{4ij}{i^2 - j^2}\right) v & \text{if } i + j = 2n + 1, \end{cases}$$

$$k_{ij} = \begin{cases} \dfrac{j^2\pi^2}{2}(1 - v^2) & \text{if } i = j, \\ 0 & \text{if } i \neq j \text{ and } i + j = 2n, \\ \left(\dfrac{2ij}{i^2 - j^2}\right) \eta v & i + j = 2n + 1. \end{cases}$$

The results of numerical analysis for the maximum normalized vibration amplitude with different damping factors η_d are plotted in Figure 5. As shown in the figure, the

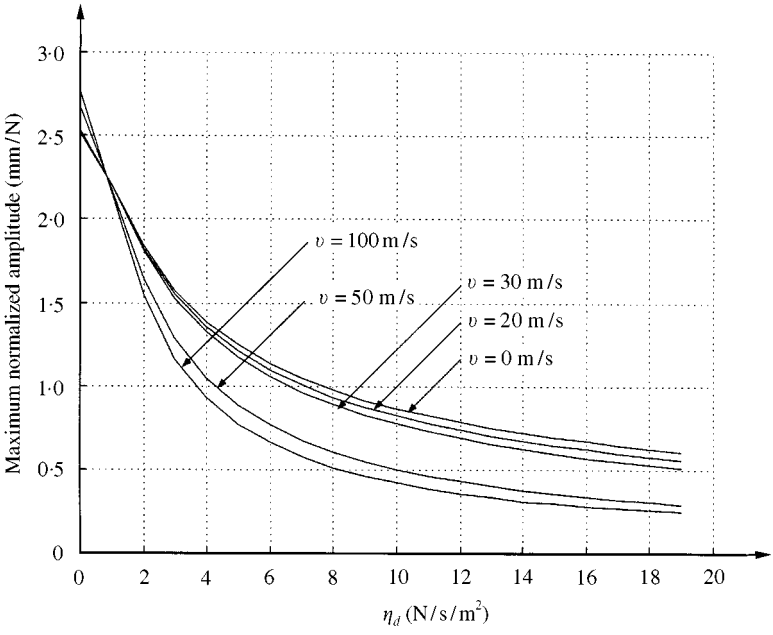

Figure 5. Maximum vibration amplitude with different damping factors under different wire speeds with wire tension at $P = 20$ N.

amplitude is reduced to approximately $\frac{1}{5}$ of the non-damped vibration as η_d is increased to 19 Ns/m^2. Such drop-off is more pronounced when the speed of wire, v, is larger.

4. DISCUSSIONS

In this paper, we presented the results of vibration analysis in the free abrasive machining (FAM) of the wiresaw manufacturing process. In the analysis, we treat the abrasive grits in the slurry as excitations to the wire to cause vibrations via the "rolling-indenting" process. The results of single and multiple excitations are presented with both closed form and numerical results. It is shown that both the closed form and numerical results match with each other very closely. The single excitation gives rise to a more sharp normalized vibration amplitude (amplitude per applied force) than that of multiple excitations. Both vibration patterns exhibit the typical behaviors of interference of two frequencies (wire's fundamental frequency and excitation frequency) when they are close to each other. In the figures plotted, the twin-peak displacement profile is a result of the excitation frequency being 20% of the fundamental frequency.

When the vibration analysis is based on multiple excitations, we found that the maximum amplitude of vibration will asymptotically approach a steady state value once the number of excitations reaches 50 or more. In a practical slicing process, there will be more than 50 abrasive particles making contact with the surface at any given time typically. This result is very significant because it suggests that a steady

state amplitude of vibration can be used in the analysis of wire vibration for the purpose of predicting the kerf loss.

For small vibration, the equations of motion in the horizontal direction and the vertical direction are the same so that the results are equally applicable to the vibration in the horizontal direction. While the vibration in the horizontal direction will result in kerf loss, the vibration in vertical direction facilitates the "rolling-indenting" process, and hence the removal of materials.

In order to reduce the kerf loss, the amplitude of vibration of the wiresaw manufacturing process needs to be minimized across a spectrum of excitation frequencies. The analysis of frequency response reveals that it is more effective to increase the tension of wire for reducing the vibration amplitude and kerf loss than to change the speed of wire. When the tension is increased, the stiffness of the system is also increased — resulting in reduction of kerf loss [6]. In recent industrial practice where tension of wire is increased, the quality and effectiveness of slicing process are both enhanced. It is also very crucial in the design of wiresaws to realize that the amplitude of vibration is not sensitive to the changes in wire speed, especially when the speed is below 25 m/s, although increase in wire speed will affect other results such as materials removal rate.

The damped vibration is obtained numerically with respect to various damping factors and speed of wire. As expected, when the damping factor increases, the amplitude of vibration will decrease. Such decrease in amplitude of vibration is more rapid when the speed of wire is larger. Due to the hydrodynamic effect of slurry in the wiresaw cutting process, it is desirable to have slurry that is neither too viscous nor too diluted [2, 14]. On the other hand, the amplitude of vibration will be too excessive if the damping factor, η_d, is too small. A different carrier for slurry may be used to achieve a certain desirable damping factor and hydrodynamic effect for slicing.

5. CONCLUSIONS

We present the results of analysis of vibration and frequency responses of wire vibrations for industry wiresaw system. Both closed form and numerical solutions of vibration due to single and multiple excitations are presented and discussed. Due to the small mass density of the wire under high tension, it is practically impossible for the industrial wiresaw to experience the divergence instability because most wiresaw systems operate at a speed significantly lower than the critical speed for instability.

From the results of this paper, there are two ways by which the vibration and kerf loss can be reduced: (1) increase the tension of wire, and (2) increase the damping factor of the abrasive slurry. Analysis in frequency responses reveals that the tension of wire is the most significant factor that affects the vibration amplitude. A small variation in tension will result in considerable change in vibration amplitudes. On the other hand, the speed of wire is not a contributing factor to the vibration of the wire when the speed of the wire is below 25 m/s. The damping effects, due to the viscous slurry in which the wire is immersed, can reduce the vibration amplitudes. However, the damping factor needs to be determined in conjunction with the hydrodynamic nature of the slurry.

ACKNOWLEDGMENT

The research has been supported by NSF (Grant No. DMI-9634889) and a DoE SBIR Phase II grant (DoE DE-FG02-95ER81978) through GT Equipment Technologies.

REFERENCES

1. I. Kao, S. Wei and F.-P. Chiang 1998 *NSF Disign and Manufacturing Grantees Conferencs*, 427–428. Vibration of wiresaw manufacturing processes and wafer surface measurement.
2. I. Kao, V. Prasad, F. P. Chiang, M. Bhagavat, S. Wei, M. Chandra, M. Costantini, P. Leyvraz, J. Talbott and K. Gupta 1998 *The Eighth International Symposium on Silicon Material Science and Technology*. Modeling and experiments on wiresaw for large silicon wafer manufacturing.
3. J. Li, I. Kao and V. Prasad 1998 *ASME Journal of Electronics Packaging* **120**, 123–128. Modeling stresses of contacts in wiresaw slicing of polycrystalline and crystalline ingots: Application to silicon wafer production.
4. J. A. Wickert and C. D. Mote 1998 *Shock Vibration Digest* **20**, 3–13. Current research on the vibration and stability of axially moving materials.
5. J. A. Wickert and C. D. Mote 1990 *ASME Journal of Applied Mechanics* **57**, 738–744. Classical vibration analysis of axially moving continua.
6. J. A. Wickert and C. D. Mote 1991 *ASME Applied Mechanics Review* **44**, S279–S284. Response and discretization methods for axially moving materials.
7. M. Pakdemirli, A. G. Ulsoy and A. Ceranoglu 1994 *Journal of Sound and Vibration* **169**, Transverse vibration of an axially accelerating string.
8. F. Y. Huang and C. D. Mote 1995 *Journal of Sound and Vibration* **181**. On the translating damping caused by a thin viscous fluid layer between a translating string and a translating rigid surface.
9. S. Ying and C. A. Tan 1996 *Journal of Vibration and Acoustics* **118**. Active vibration control of the axially moving string using space feedforward and feedback contollers.
10. R. D. Swope and W. F. Ames 1963 *Journal of Franklin Institute* **275**, 36–55. Vibration of a moving threadline.
11. F. R. Archibald and A. G. Emslie 1958 *ASME Journal of Applied Mechanics* **25**, 347–348. The vibration of a string having a uniform motion along its length.
12. L. Meirovitch 1974 *AIAA Journal* **12**, 1337–1342. A new method of solution of the eigenvalue problem for gyroscopic systems.
13. L. Meirovitch 1975 *ASME Journal of Applied Mechanics* **42**, 446–450. A modal analysis for the response of linear gyroscopic systems.
14. M. Bhagavat, V. Prasad and I. Kao 1998 Elasto-hydrodynamic interaction in the free abrasive wafers slicing using a wiresaw: modeling and finite element analysis (submitted).
15. Leonard Meirovitch 1997 *Principles and Techniques of Vibrations*. Englewood-Cliffs, NJ: Prentice-Hall.
16. R. K. Sahoo, V. Prasad, I. Kao, J. Talbott and K. Gupta 1998 *ASME Journal of Electronics Packaging* **120**. An integrated approach for analysis and design of wafer slicing by a wire saw.

APPENDIX A NOMENCLATURE

ρ, L, P	mass density per unit length (g/m), length (mm), and tension (N) of wire
U, V	transverse displacement (mm), and translating speed (m/s) of wire

F, f	external excitation per unit length (N/mm), and non-dimensionalized excitation force (FL/P)
f_0, ω	non-dimensionalized amplitude, and frequency of single-particle harmonic excitation
f_{0_j}, ω_{f_j}	non-dimensionalized amplitude, and frequency of jth harmonic excitation
ω_n, Ω_n	non-dimensionalized, and realistic frequency of the nth natural modes of wire
ω_1	the fundamental frequency of wire
F_η	damping force (N/mm)
u, v	non-dimensionalized transverse displacement (U/L), and translating speed of wire ($V\sqrt{\rho/P}$)
t, x	non-dimensionalized time ($T\sqrt{(P/\rho L^2)}$), and horizontal co-ordinate (X/L)
η_d, η	damping factor (N_s/mm^2), and non-dimensionalized damping factor ($\eta_d L/\sqrt{\rho P}$)